

Pressure Dependence of the Microwave Resonance Properties of Some Spinel and Garnet Ferrites*†

I. P. KAMINOW‡ AND R. V. JONES

Gordon McKay Laboratory, Harvard University, Cambridge, Massachusetts

(Received March 15, 1961)

The anisotropy field, g value, and linewidth of several spinel and garnet ferrites have been measured at X band and room temperature as functions of hydrostatic pressure to 10^4 kg/cm². The crystals studied include yttrium, ytterbium, and erbium iron garnet; magnesium ferrite (with different distributions of Mg²⁺ ions on A and B sites); and Ni_{1-z}Co_zFe₂O₄ with $z=0, 0.05$ and 0.10 . The pressure dependence of magnetization was measured using magnetostatic mode methods in the narrow linewidth materials, yttrium iron garnet and magnesium ferrite.

The complexity of the crystal structure and magnetic interactions makes any quantitative interpretation very difficult.

INTRODUCTION

THE two dominant factors determining the magnetic properties of ferrimagnetic oxides, the superexchange and crystalline field interactions, are sensitively related to the interionic spacings in the crystalline unit cell. When hydrostatic pressure is applied to a cubic crystal, such as a spinel or garnet ferrite, the unit cell will remain cubic (provided no phase change occurs¹) and the lattice constant will be reduced in proportion to the compressibility. As a result of the compression, one would expect the superexchange interaction, which arises from the overlap of neighboring wave functions, to become more pronounced. Moreover, the crystalline electric fields at the metal ions, produced by neighboring oxygen ions, would also be expected to increase in intensity. Changes in local crystalline fields would be manifested mainly by

However, the observations can be understood qualitatively in terms of the volume dependence of the crystalline fields and the exchange interactions. In the case of erbium iron garnet, the volume dependence of the ferric-rare-earth exchange constant is calculated; and, in the case of nickel cobalt ferrite, a simple explanation is offered for the observed volume dependence of the Co²⁺ anisotropy.

The contribution of thermal lattice vibrations to the linewidth in yttrium iron garnet is discussed, and the possibility of an anisotropic spin-orbit interaction is considered.

variations in magnetic anisotropy, and changes in superexchange fields would cause variations in magnetization. These macroscopic properties, magnetization and anisotropy, as well as g value and linewidth, can be measured at room temperature to 10^4 kg/cm² (about 10^4 atm) with the high-pressure microwave resonance apparatus described below. It is found that the 0.2% reduction in lattice constant occurring in the ferrites at 10^4 kg/cm² produces rather large changes in the resonance properties.

Although the prospect of varying the exchange and crystalline field interactions directly is quite attractive, a number of difficulties arise in analyzing the results of pressure measurements. Despite the fact that the pressure dependence of the lattice constant may be determined from the compressibility by symmetry considerations, the pressure dependence of the oxygen parameters, which determine the relative positions of oxygen ions in the complex unit cell, cannot be determined except by x-ray analysis at high pressure. The simplest assumption, which is often a poor approximation, is to suppose that all interionic distances vary in proportion to the compressibility, i.e.,

$$(\partial \ln \xi / \partial P) = \frac{1}{3} (\partial \ln v / \partial P) = -\frac{1}{3} \chi, \quad (1)$$

* Supported by an Air Force contract.

† Based on a thesis presented by I. P. K. to the Division of Engineering and Applied Physics, Harvard University, Cambridge, Massachusetts, May 1960, in partial fulfillment of the requirement for the degree of Doctor of Philosophy.

‡ Now at Bell Telephone Laboratories, Holmdel, New Jersey.

¹ Experimentally, no abrupt changes, no hysteresis, and no variations in symmetry of measured quantities are observed as a function of pressure.

where ξ is an arbitrary spacing, v is the volume, P the pressure, and χ the compressibility. Using a point-charge model, one may then estimate the pressure variation of a cubic crystalline potential,

$$V_{\text{cu}} \propto \langle r^4 \rangle R^{-6} = \langle r^4 \rangle v^{-5/3}, \quad \partial \ln V_{\text{cu}} / \partial P = (5/3)\chi, \quad (2)$$

where $\langle r^4 \rangle$ is the fourth moment of the radial wave function for the central ion and R is the separation between the central metal ion and neighboring oxygen ions. In the preceding estimate, it is assumed that $\langle r^4 \rangle$ is pressure independent, that crystalline field components of lower symmetry are not introduced by the applied isotropic stress and that V_{cu} satisfies Laplace's equation. The validity of these assumptions is open to question.

Several experiments and calculations suggest that the radial wave functions are quite different for a free ion and for an ion in a crystal lattice.²⁻⁴ Thus, $\langle r^4 \rangle$ depends upon the proximity of neighboring ions. The magnitude of the pressure dependence of $\langle r^4 \rangle$ is not known although one may infer from a neutron diffraction experiment² on Mn^{2+} in several different host crystals that the variation will be small for a 0.2% change in lattice constant.

Walsh has shown,⁵ in a high-pressure paramagnetic resonance study, that the various symmetry components of the local crystalline field vary at different rates in nickel fluosilicate, i.e., the cubic portion changes slowly while the axial part varies rapidly with pressure. Finally, the assumption of the applicability of Laplace's equation implies no overlap of oxygen and metal ion wave functions, a situation which cannot obtain in a ferrimagnet where superexchange is important.

It is difficult to correlate the observed pressure dependences of macroscopic ferrimagnetic properties with recent microscopic theories for anisotropy, g value, linewidth, and magnetization because of the multiplicity of pressure dependent variables. Aside from the additional pressure dependent unknowns introduced by variations in the oxygen parameters, it is necessary to determine the variation of the sublattice properties from a measurement of a single macroscopic pressure shift. With the small pressure range available, pressure induced variations are usually linear so that, unlike the analysis of temperature measurements, it is not possible to deduce the sublattice properties by curve fitting. This latter difficulty may be overcome by a combined temperature-pressure experiment or, as we have done in certain cases, by studying materials as a function of pressure and composition. For example, in the rare-earth garnets, the pressure dependence of the rare-earth sublattice properties may be estimated by subtracting the pressure dependence of the ferric sublattices as

² J. M. Hastings, N. Elliott, and L. M. Corliss, *Phys. Rev.* **115**, 13 (1959).

³ W. Marshall, *Bull. Am. Phys. Soc.* **4**, 142 (1959).

⁴ A. J. Freeman and R. E. Watson, *Phys. Rev.* **118**, 1168 (1960).

⁵ W. M. Walsh, Jr., *Phys. Rev.* **114**, 1475, 1485 (1959).

determined from measurements on yttrium iron garnet. Also, the contribution of Co^{2+} in $\text{Ni}_{1-z}\text{Co}_z\text{Fe}_2\text{O}_4$ may be determined from measurements on NiFe_2O_4 for small z .

In the following sections, we will describe high pressure microwave resonance experiments on yttrium, erbium, and ytterbium iron garnets (YIG, ErIG, and YbIG); MgFe_2O_4 with variable distribution of Mg^{2+} ions; and $\text{Ni}_{1-z}\text{Co}_z\text{Fe}_2\text{O}_4$ with variable z .

APPARATUS

Microwave magnetic resonance is observed by measuring the input standing wave ratio (VSWR) of a reflection-type cavity, with the aid of a pair of directional couplers, as a function of applied magnetic field.⁶ The cavity is resonant in the X band and is of the cylindrical TE_{011} variety. The rf magnetic field, h_{rf} , is in the axial direction on the cylinder axis on which the sample is located. Single-crystal samples are oriented with a $[110]$ direction along the cavity axis. The cavity is situated in the gap of a rotating magnet with the rotation axis along the cavity axis. The dc magnetic field, H_{dc} , is always normal to h_{rf} and may be rotated into coincidence with the principal crystal directions $[100]$, $[111]$, $[110]$. From measurements of the field for resonance in these three directions, one may calculate⁷ an effective g value, g_{eff} , and the first- and second-order anisotropy fields, K_1/M and K_2/M . One may also measure the linewidths, ΔH , in the principal directions.

Magnetostatic mode methods⁸ are employed to measure the magnetization, M . The sample is located at a position of vanishing h_{rf} , and H_{dc} is rotated so as to permit appropriate modes to be excited.

The high-pressure resonance apparatus is illustrated schematically in Fig. 1. The entire cavity is immersed in a fluid (pentane) under hydrostatic pressure. The fluid is pumped through a flexible stainless steel tube into a cylindrical beryllium-copper vessel⁹ or "bomb." The outer diameter of the bomb (2 in.) is prescribed by the magnet gap and the inner diameter ($\frac{1}{16}$ in.) by considerations of mechanical strength. In order that the X -band cavity be small enough to fit into the bomb, it is filled with alumina (Coors AD-99) which, in addition to having a high dielectric constant ($\epsilon=9.3$), is not very compressible and has a high dielectric Q ($\tan\delta=1.4 \times 10^{-4}$). The alumina dielectric filler fits into an aluminum shell which screws onto the "microwave plug" that seals⁹ one end of the cylindrical bomb. The cavity is loop-coupled to a coaxial line contained in the

⁶ J. O. Artman and P. E. Tannenwald, *J. Appl. Phys.* **26**, 1124 (1955).

⁷ J. F. Dillon, S. Geschwind, and V. Jaccarino, *Phys. Rev.* **100**, 750 (1955).

⁸ J. F. Dillon, Jr., *Phys. Rev.* **112**, 59 (1958); R. L. White, *J. Appl. Phys.* **31**, 86S (1960).

⁹ W. Paul, G. B. Benedek, and D. M. Warschauer, *Rev. Sci. Instr.* **30**, 874 (1959).

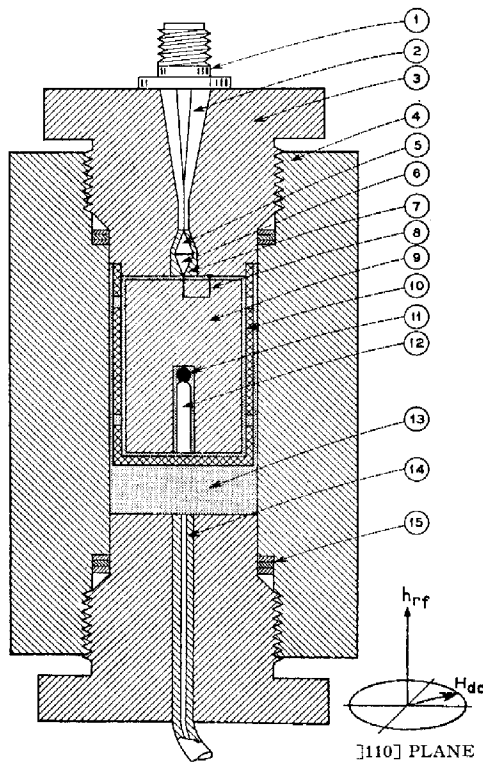


FIG. 1. Schematic drawing of the high pressure resonance apparatus (not to scale): 1, coaxial connector; 2, tapered transition; 3, microwave plug; 4, beryllium copper bomb; 5, beryllium copper cone; 6, brass cone; 7, synthetic mica dielectric; 8, coupling loop; 9, alumina dielectric; 10, cavity wall; 11, sample; 12, quartz mounting rod; 13, pressure fluid; 14, pressure fluid input tubing; 15, sealing washers.

plug. The coaxial line is tapered to match a standard type *N* connector.

A pressure seal in the coaxial line is provided by a small beryllium copper cone that forms a portion of the center conductor and is seated in a thin conical shell of dielectric material (synthetic mica, Brush Beryllium Company) which in turn is seated in a

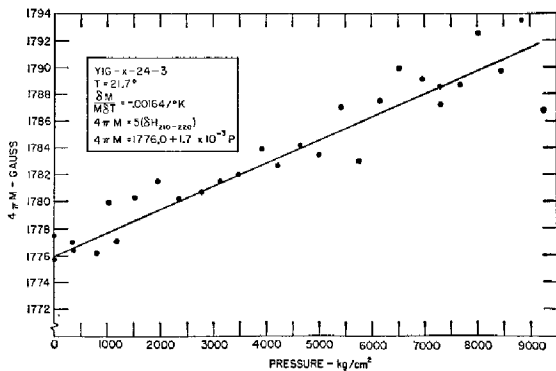


FIG. 2. Pressure dependence of magnetization in yttrium iron garnet.

conical cavity in the plug.^{10,11} A small brass cone with its base adjacent to the base of the beryllium copper cone is employed to reduce the electrical mismatch.

The pressure fluid circulates freely throughout the cavity and around the sample via the small spaces between the various segments comprising the cavity and through holes in the cavity wall.

The oriented sample, a small polished sphere (0.010–0.025 in. diam) is adhered to a quartz rod by a thin layer of resin (Stycast 2661) in order not to introduce significant non-hydrostatic stresses. The rod slides into a hole along the cavity axis where the rf electric field vanishes. In the case of magnetostatic mode measurements, an off-center hole parallel to the cavity axis is made so that the sample is situated at a point of vanishing h_{rf} . The sample is placed in the hole and an alumina rod is pushed up behind it so that the sample is free to rotate.

All measurements are made at room temperature which may vary by a few degrees C during a pressure run. In certain cases, the temperature deviation is corrected for using the temperature derivative at atmospheric pressure. In general, the pressure measurements can be represented by a linear least-squares fit for the small pressure range available. The experimental results are given in terms of the least squares equation along with the calculated standard deviations for the coefficients to indicate the scatter in the data.

EXPERIMENTAL RESULTS

Yttrium Iron Garnet¹²

The magnetization of yttrium iron garnet increases 0.96% in 10^4 kg/cm² (Fig. 2),

$$4\pi M = 1776.0 \pm 0.5 + (1.7 \pm 0.1) \times 10^{-3} P \text{ (gauss), } (3)$$

where the error given is the calculated standard deviation, P is in kg/cm² and $T = 22^\circ\text{C}$. Most of the

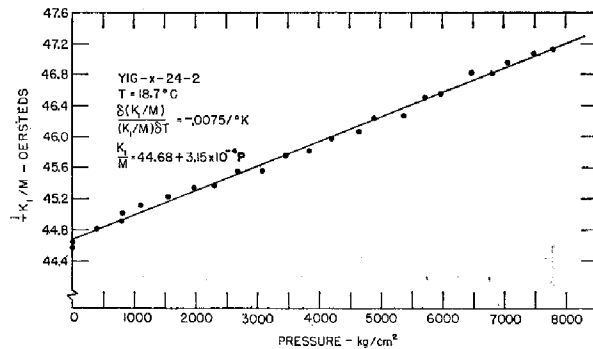


FIG. 3. Pressure dependence of first-order anisotropy field in yttrium iron garnet.

¹⁰ P. W. Bridgman, *The Physics of High Pressure* (G. Bell and Sons, London, 1952).

¹¹ W. M. Walsh, Jr., and N. Bloembergen, *Phys. Rev.* **107**, 904 (1957).

¹² I. P. Kaminow, W. Paul, and R. V. Jones, *Bull. Am. Phys. Soc.* **4**, 177 (1959). (Values quoted are in error. See text.)

pressure shift can be attributed to the explicit volume dependence of M , $M=N\mu/v$, where μ is the moment per formula unit, N the number of formula units in a unit volume. With a compressibility¹³ of 0.61% for 10^4 kg/cm², μ increases by 0.35% in 10^4 kg/cm²; in terms of volume,

$$(\partial \ln M / \partial \ln v) = -1.57, \quad (\partial \ln \mu / \partial \ln v) = -0.57. \quad (4)$$

The anisotropy field increases 7.05% in 10^4 kg/cm² (Fig. 3),

$$-K_1/M = 44.68 \pm 0.02 + (3.15 \pm 0.05) \times 10^{-4} P \text{ (oe)}, \quad (5)$$

at $T=19^\circ\text{C}$. The second-order field remains small, $|K_2/M| < 1$ oe. Eliminating M and taking into account the explicit volume dependence of K_1 , we find

$$\partial \ln k_1 / \partial \ln v = -12.1, \quad (6)$$

where k_1 is the anisotropy constant per formula unit.

From the crystalline field theories of ferrimagnetic anisotropy developed by Yosida and Tachiki¹⁴ and Wolf,¹⁵ one obtains, for cubic fields,

$$k_1 = \nu_a \delta_a a_a r(y_a) + \nu_d \delta_d a_d r(y_d), \quad (7)$$

for the ferric a and d sublattices. Here ν_a and ν_d are the number of a or d ions per formula unit; δ_a and δ_d are averaging factors (less than unity) which account for the fact that the cubic axes of the local fields for ions on a given sublattice in a unit cell are not parallel; a_a and a_d are the cubic field splitting parameters; $r(y_a)$ and $r(y_d)$ are functions of the sublattice magnetizations. The last three factors in each term are all likely to be pressure dependent. If it is supposed that only a_a and a_d are pressure dependent and that they

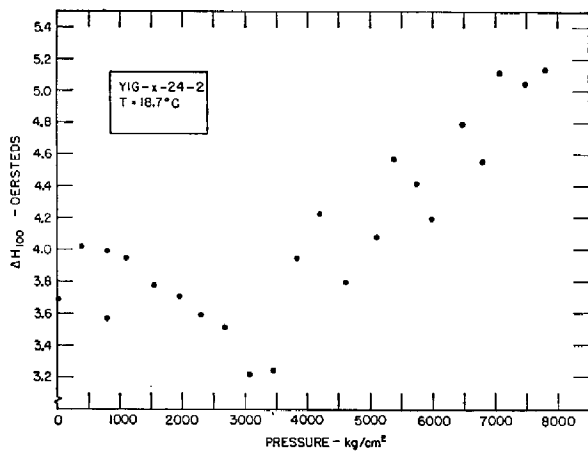


FIG. 4. Pressure dependence of linewidth in the [100] direction in yttrium iron garnet. The results for [110] and [111] are practically the same as for [100].

¹³ A. E. Clark and R. G. Strakna, J. Appl. Phys. (to be published).

¹⁴ K. Yosida and M. Tachiki, Progr. Theoret. Phys. (Kyoto) 17, 331 (1957).

¹⁵ W. P. Wolf, Phys. Rev. 108, 1152 (1957).

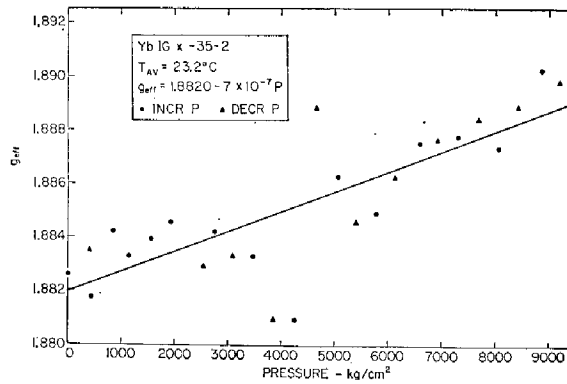


FIG. 5. Pressure dependence of g_{eff} in YbIG.

vary in the same way, then, from the point charge model, it is found that the effective a varies as the sixth power of cubic field, V_{ou} . This rough result may be compared with the theory of Watanabe¹⁶ which predicts a second power dependence and the experiments of Walsh¹⁷ which show a fourth power dependence.

It has been shown^{18,19} that one cannot neglect the F (fourth degree axial) terms in the expression for k_1 as we have done in (7). The F terms will exhibit an unknown pressure dependence due to the unknown variations of the oxygen parameters. The variation in k_1 is probably dominated by changes in the F terms.

The g factor is practically independent of pressure:

$$g_{\text{eff}} = 2.010 \pm 0.001 + (7 \pm 8) \times 10^{-8} P. \quad (8)$$

The observed linewidth behavior is rather curious and cannot be represented by a straight line (see Fig. 4). For the degree of polishing used, the linewidth is governed by surface roughness.²⁰

Ytterbium and Erbium Iron Garnets

The pressure derivatives of g_{eff} are of opposite sign in YbIG (Fig. 5) and ErIG (Fig. 6) and the magnitude of the derivative is considerably larger in ErIG:

$$\text{YbIG: } g_{\text{eff}} = 1.8820 \pm 0.0006 + (7.5 \pm 1.1) \times 10^{-7} P, \quad (9)$$

$$\text{ErIG: } g_{\text{eff}} = 1.431 \pm 0.002 - (2.4 \pm 0.4) \times 10^{-6} P. \quad (10)$$

The temperature for YbIG measurements is 23°C and for ErIG 31°C . Paramagnetic resonance studies²¹ of

¹⁶ H. Watanabe, Progr. Theoret. Phys. (Kyoto) 18, 405 (1957); Phys. Rev. Letters, 4, 410 (1960). Also M. J. D. Powell, J. R. Gabriel, and D. F. Johnston, Phys. Rev. Letters 5, 145 (1960).

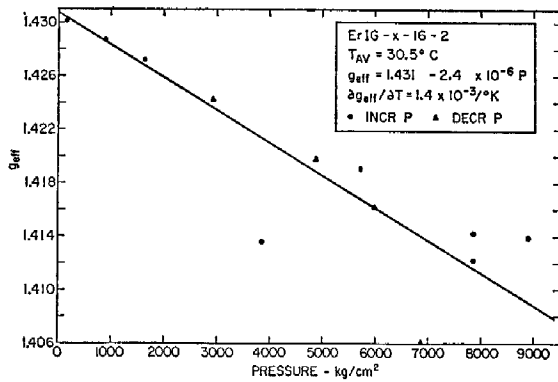
¹⁷ W. M. Walsh, Jr., Phys. Rev. Letters 4, 507 (1960); Phys. Rev. 122, 762 (1961).

¹⁸ S. Geschwind, Phys. Rev. Letters 3, 207 (1959); Phys. Rev. 121, 363 (1961).

¹⁹ G. P. Rodrigue, H. Meyer, and R. V. Jones, J. Appl. Phys. 31, 376S (1960).

²⁰ R. C. LeCraw, E. G. Spencer, and C. S. Porter, Phys. Rev. 110, 1311 (1958).

²¹ M. Ball, G. Garton, M. J. M. Leask, D. Ryan, and W. P. Wolf, J. Appl. Phys. 32, 267S (1961).

FIG. 6. Pressure dependence of g_{eff} in ErIG.

rare earths in gallium and aluminum garnets also indicate that Er^{3+} is much more sensitive to crystal structure than Yb^{3+} . From temperature data, ErIG appears to conform to the Kittel g -value theory while YbIG does not.¹⁹ Assuming the Kittel formula,²² $g_{\text{eff}} = (g_A/M_A)(M_A + M_B)$, to hold for ErIG, it is possible to estimate the volume dependence of M_B , the erbium sublattice magnetization, from the volume dependences of g_A and M_A , where A refers to the combined ferric sublattice, obtained from the YIG measurements,

$$\partial \ln M_B / \partial \ln v = -8.4. \quad (11)$$

(We have assumed the compressibility of ErIG to be the same as that for YIG.) If the erbium sublattice is far from saturation, then

$$M_B = \chi_B H_B = \chi_B \lambda_{AB} M_A, \quad (12)$$

in which χ_B is the susceptibility of the B sublattice and λ_{AB} is the composite ferric-rare earth exchange constant. The exchange constant increases rapidly as neighboring ions approach one another,

$$\partial \ln \lambda_{AB} / \partial \ln v = -7.0. \quad (13)$$

The anisotropy data are given by

YbIG:

$$-K_1/M = (38.0 \pm 0.2) + (5.5 \pm 0.4) \times 10^{-4} P \text{ (oe)} \quad (14)$$

$$-K_2/M = 8 \pm 4 \text{ (oe)}, \quad (15)$$

ErIG:

$$-K_1/M = (74.1 \pm 0.2) + (5.5 \pm 0.4) \times 10^{-4} P \text{ (oe)} \quad (16)$$

$$-K_2/M = 22 \pm 1 + (6 \pm 3) \times 10^{-4} P \text{ (oe)}. \quad (17)$$

The linewidths in these materials did not permit measurements of M by magnetostatic mode techniques. However, using data²³ for M at $P=0$ and estimates of the pressure variation of M obtained from the pressure shifts in g_{eff} , it is possible to estimate the rare earth

contribution to anisotropy, K_{1B} . Unlike the ferric contribution, the rare-earth contribution is positive and decreases in magnitude with pressure. The fractional variation in K_{1B} for ErIG is considerably larger than the variation for YbIG.

The linewidth increases by approximately 20% in YbIG and 15% in ErIG for 10^4 kg/cm^2 .

Magnesium Ferrite

The distribution of Mg^{2+} ions on A and B sites in MgFe_2O_4 can be controlled by heat treatment.²⁴ A particular distribution may be represented by $(\text{Mg}_x^{2+}\text{Fe}_{1-x}^{3+})[\text{Mg}_{1-x}^{2+}\text{Fe}_{1-x}^{3+}]\text{O}_4$, where x is the fraction of Mg^{2+} ions on A sites. The fraction, x , may be determined from a measurement of magnetic moment per molecule extrapolated to $T=0$.

Measurements were made on a stoichiometric crystal, grown from a flux by J. P. Remeika, for which $x=0.21$. A second crystal was annealed to give $x=0.14$.²⁵

The linewidths are sufficiently narrow to permit magnetostatic mode measurements of M

$$x=0.21: 4\pi M = 2268.1 \pm 0.6 + (2.66 \pm 0.08) \times 10^{-3} P \text{ (gauss)}, \quad (18)$$

$$x=0.14: 4\pi M = 1824 \pm 9 + (3.6 \pm 0.1) \times 10^{-3} P \text{ (gauss)}, \quad (19)$$

where $T=27^\circ\text{C}$ for $x=0.21$ and $T=22^\circ$ for $x=0.14$. These pressure shifts are somewhat larger than observed in YIG.

The anisotropy fields are

$$x=0.21: -K_1/M = 164.9 \pm 0.2 + (5.0 \pm 0.4) \times 10^{-4} P \text{ (oe)} \quad (20)$$

$$-K_2/M = -(6.3 \pm 0.4) + (3.33 \pm 0.08) \times 10^{-3} P \text{ (oe)}, \quad (21)$$

$$x=0.14: -K_1/M = 199.9 \pm 0.5 + (7 \pm 1) \times 10^{-4} P \text{ (oe)} \quad (22)$$

$$-K_2/M = 29 \pm 1 + (4.3 \pm 0.3) \times 10^{-3} P \text{ (oe)}, \quad (23)$$

where $T=26^\circ$ for $x=0.21$ and $T=25^\circ\text{C}$ for $x=0.14$. The volume derivatives are about half those observed in YIG,

$$x=0.21: \partial \ln k_1 / \partial \ln v = -5.0, \quad (24)$$

$$x=0.14: \partial \ln k_1 / \partial \ln v = -6.9. \quad (25)$$

(In the absence of compressibility data, we have assumed a 0.7% volume reduction for 10^4 kg/cm^2 .)

For the spinel structure, the local symmetry axes are parallel for all sites so that an averaging factor δ is not required [Eq. (7)]. However, although two pieces of

²⁴ C. J. Kriessman and S. E. Harrison, Phys. Rev. **103**, 857 (1956).

²⁵ The magnetization at low temperature was measured by S. Foner.

²² C. Kittel, Phys. Rev. **115**, 1587 (1959).

²³ F. Bertaut and R. Pauthenet, Proc. Inst. Elec. Engrs. (London) **B104**, 261 (1957).

data for the different distributions are available, it is still not possible to find the volume dependence of a_A and a_B separately, even if noncubic distortions are neglected, for lack of information about the variation of sublattice magnetization, i.e., $r(y_A)$ and $r(y_B)$. A simple calculation neglecting F terms and the pressure variation of $r(y_A)$ and $r(y_B)$ gives a third power dependence for $x=0.14$.

The lines are broadened with increased pressure and the g -values decrease.

$$x=0.21: g_{\text{eff}} = 1.996 \pm 0.002 - (6 \pm 1) \times 10^{-7} P, \quad (26)$$

$$x=0.14: g_{\text{eff}} = 1.9999 \pm 0.0003 - (3.8 \pm 0.6) \times 10^{-7} P. \quad (27)$$

Nickel Cobalt Ferrite²⁶

Anisotropy measurements on cobalt-doped magnetite, $\text{Fe}_{3-y}\text{Co}_y\text{O}_4$, have shown²⁷ that, for small y , the Co^{2+} contribution to anisotropy is proportional to y . The anisotropy per cobalt ion may, therefore, be determined from measurements on samples of two different compositions.

Nickel ferrite, because of its lower loss, is better suited to resonance measurements than magnetite. Crystals of $\text{Ni}_{1-z}\text{Co}_z\text{Fe}_2\text{O}_4$ were grown by the flux method with the intended concentrations $z=0, 0.05$, and 0.10 . The pressure dependences of the anisotropy fields are

$$z=0: K_1/M = -236.6 \pm 0.03 - (1.06 \pm 0.05) \times 10^{-3} P \text{ (oe)} \quad (28)$$

$$K_2/M \approx 28 \text{ (oe)}, \quad (29)$$

$$z=0.05: K_1/M = 64.7 + 0.9 - (1.9 \pm 0.2) \times 10^{-3} P \text{ (oe)} \quad (30)$$

$$K_2/M = -323 \pm 2 + (0.0 \pm 0.3) \times 10^{-3} P \text{ (oe)}, \quad (31)$$

$$x=0.10: K_1/M = 322 \pm 2 - (2.5 \pm 0.3) \times 10^{-3} P \text{ (oe)} \quad (32)$$

$$K_2/M = -528 \pm 4 - (1.8 \pm 0.7) \times 10^{-3} P \text{ (oe)}, \quad (33)$$

where $T=28, 24^\circ\text{C}$ for $z=0, 0.05$, respectively.

The relatively large linewidths did not permit measurements of magnetization. However, from measurements on polycrystalline nickel cobalt ferrite by C. Nowlin, we estimate $M=257, 273$, and 290 gauss for $z=0, 0.05$, and 0.10 , respectively, at $P=0$.

The linear relation,

$$K_{1,2}(z) = zK_{1,2}(\text{Co}) + (1-z)K_{1,2}(0), \quad (34)$$

²⁷ L. R. Bickford, J. M. Brownlow, and R. F. Penoyer, Proc. Inst. Elec. Engrs. (London), **B104**, 5, 238S (1957).

²⁶ I. P. Kaminow, J. Appl. Phys. **31**, 220S (1960).

in which $K_{1,2}(z)$ is the measured anisotropy constant for $\text{Ni}_{1-z}\text{Co}_z\text{Fe}_2\text{O}_4$, $K_{1,2}(\text{Co})$ is the Co^{2+} contribution and $K_{1,2}(0)$ is the NiFe_2O_4 contribution, is found to hold reasonably well for the preceding measurements. For the cobalt contribution, we find

$$K_1(\text{Co}) \approx 1.6 \times 10^6 \text{ erg/cc}, \quad (35)$$

$$K_2(\text{Co}) \approx -1.6 \times 10^6 \text{ erg/cc}. \quad (36)$$

The constants²⁸ are nearly an order of magnitude smaller than those found for Co^{2+} in magnetite.²⁷ A similar reduction in cobalt contribution is found for cobalt doped manganese ferrite.^{27,29}

The cobalt contribution to the anisotropy of $\text{Co}_y\text{Fe}_{3-y}\text{O}_4$ has been explained by Slonczewski.³⁰ If Co^{2+} ions are located on widely separated octahedral sites and no distinction is made between Fe^{2+} and Fe^{3+} ions, the crystalline field is cubic with a small trigonal distortion along a $[111]$ axis. In this situation the ground state of Co^{2+} is an orbital doublet with effective angular momentum $\pm\alpha\mathbf{k}$, where \mathbf{k} is a unit vector along the trigonal direction and α lies in the range $1 < \alpha < \frac{3}{2}$. The ground state wave function, having trigonal symmetry, fits snugly into the trigonal surroundings, and the orbital angular momentum is constrained to lie along the trigonal axis. The fact that the orbital moment is not quenched gives rise to large ferrimagnetic anisotropy. The anisotropy of the "locked in" orbital wave function is impressed upon the spin (which accounts for most of the magnetic moment) via the spin-orbit interaction $\lambda\mathbf{L}\cdot\mathbf{S}$, where λ is the spin-orbit constant.

Slonczewski's expressions for $K_1(\text{Co})$ and $K_2(\text{Co})$ involve only the parameter $|\alpha\lambda|$, representing the magnitude of the spin-orbit interaction. From our data, we find $|\alpha\lambda| \approx 74 \text{ cm}^{-1}$ which is about half the value calculated for magnetite, i.e., $|\alpha\lambda| = 132 \text{ cm}^{-1}$. In either case, if λ is taken to be the free ion value, -176 cm^{-1} , α does not fall within the prescribed range $1 < \alpha < \frac{3}{2}$. For the magnetite case, the discrepancy may result from simplifications in the calculation whereby higher levels are neglected.^{30,31} It is also possible that the crystalline λ is considerably smaller than the free ion value.³²

Still another possibility is the effect of additional lower symmetry crystalline field components introduced by the clustering of Co^{2+} ions or by the differences in Fe^{2+} and Fe^{3+} ions.³⁰ In magnetite, the ferric and ferrous ions are distributed at random on B sites neighboring the cobalt ion under consideration. However, it is believed³⁰ that the electron exchange between

²⁸ The fact that K_1 and K_2 are similar in magnitude suggests that higher order terms (K_3 , etc.) may be required for a complete description.

²⁹ R. F. Pearson, Proc. Phys. Soc. (London) **A74**, 505 (1959).

³⁰ J. C. Slonczewski, Phys. Rev. **110**, 1341 (1958).

³¹ J. H. VanVleck, J. phys. radium **20**, 124 (1959).

³² J. Owen, Proc. Roy. Soc. (London) **227**, 183 (1955).

Fe^{2+} and Fe^{3+} is sufficiently rapid to make the crystal-line field appear to have the cubic plus trigonal potential assumed. In nickel ferrite, on the other hand, this argument does not hold and the randomly distributed Ni^{2+} and Fe^{3+} ions may introduce additional lower symmetry components.

From the pressure measurements on nickel cobalt ferrite, we calculate³³

$$\partial \ln(\alpha\lambda)/\partial \ln v \sim 1.1, \quad (37)$$

on the assumption that $\partial \ln M/\partial P \sim -\partial \ln v/\partial P$ as suggested by the earlier magnetization measurements on YIG and MgFe_2O_4 . The above result suggests that, if λ is volume independent, α is proportional to the first power of volume. This linear dependence may be explained on the basis of an additional crystalline field component, such as an axial potential V_a directed normal to the trigonal axis, and introduced by the neighboring Ni^{2+} and Fe^{3+} ions. Then $V_a \propto \langle r^2 \rangle / R^{-3} \propto v^{-1}$. If we consider V_a to be a perturbing potential, then the orbital doublet will be split slightly in proportion to V_a and the effective moment α will be inversely proportional to the splitting, Δ , since a second order perturbation calculation is required with no orbital degeneracy. Therefore, the effective orbital moment is

$$\alpha \propto 1/\Delta \propto V_a^{-1} \propto v^1, \quad (38)$$

as required. This mechanism may be responsible for much of the reduction in cobalt anisotropy found for Co^{2+} in nickel and manganese ferrite. Slonczewski³⁴ has proposed a different explanation, involving a reduction in the exchange field acting on Co^{2+} in ferrites other than magnetite, which appears to contradict our measurements if the exchange field is assumed to increase with pressure.

The observed pressure dependence of g_{eff} in NiFe_2O_4 ($z=0$) is unusual in that g_{eff} increases from 2.209 at $P=0$ to 2.212 at $5 \times 10^3 \text{ kg/cm}^2$ and then decreases to 2.209 at 10^4 kg/cm^2 . For the other samples,

$$z=0.05: g_{\text{eff}} = 2.215 \pm 0.001 - (5 \pm 2) \times 10^{-7} P, \quad (39)$$

$$z=0.10: g_{\text{eff}} = 2.26 \pm 0.08 + (0 \pm 2) \times 10^{-5} P. \quad (40)$$

In all cases, the linewidth increases with pressure.

DISCUSSION

Interpretation of the foregoing pressure measurements is hampered by a lack of knowledge of the pressure dependence of the oxygen parameters and by the large numbers of pressure dependent parameters encountered. However, it has been possible to separate out the pressure dependence of the exchange constant λ_{AB} for ErIG and the pressure dependence of the

cobalt anisotropy in $\text{Ni}_{1-z}\text{Co}_z\text{Fe}_2\text{O}_4$. A simple explanation for the decrease in cobalt anisotropy with pressure has been offered.

Spin-Orbit Coupling

The spin-orbit interaction plays a central role in determining the ferrimagnetic anisotropy since it provides the coupling between the nearly spin-only magnetization and the orbital moment which is coupled to the lattice by crystalline fields. The spin-orbit term has the form³⁵ $\mathbf{s} \cdot (\nabla V \times \mathbf{p})$, in which \mathbf{s} , V , and \mathbf{p} are the spin, electric field potential and momentum, respectively, of the electron. If V is the centrosymmetric Coulomb potential due to the shielded nucleus, then the spin orbit term has the familiar $\lambda \mathbf{l} \cdot \mathbf{s}$ form with $\lambda \propto \langle r^{-3} \rangle$. The increase in $\langle r \rangle$ for the crystalline ion as opposed to the free ion mentioned in the Introduction suggests that $\langle r \rangle$ will increase with pressure and λ will decrease. Comparison of the free ion and crystalline spin-orbit constants shows that λ for the transition elements is roughly 15 to 40% smaller in the crystal.³²

It is generally assumed that the portion of V contributed by the nonisotropic crystalline fields has little effect on the spin-orbit interaction because $\langle r \rangle / R$ is believed to be small enough that the magnetic electron spends most of the time near its nucleus where the central ion potential dominates.³⁶ In the light of the large overlap of central and ligand ion wave functions observed² and indicated by the strong superexchange in the spinel and garnet ferrites, it is conceivable that the crystalline fields make a significant contribution. The spin-orbit interaction would then exhibit the symmetry of the crystalline field; i.e., an anisotropic spin-orbit term would result.

If the nonisotropic crystalline field potential V_{cr} , can be factored into a radial part, $P(r)$, and an angular part, $\Omega(\theta, \varphi)$, then the contribution to the spin-orbit interaction is

$$\mathbf{s} \cdot (\nabla V_{\text{cr}} \times \mathbf{p}) = (P' \Omega / r) \mathbf{l} \cdot \mathbf{s} + (P \nabla \Omega \times \mathbf{p}) \cdot \mathbf{s}. \quad (41)$$

The first term has the usual $\mathbf{l} \cdot \mathbf{s}$ form but the spin-orbit coefficient is now a function of the electron coordinates having the symmetry of V_{cr} . The magnitude of the term depends upon the size of the radial derivative of V_{cr} at the electron. If such a term were used in a perturbation calculation for the level splittings, say, its qualitative effect could not be distinguished from a second order perturbation calculation involving both V_{cr} and the usual spin-orbit interaction. Such a term, however, might prove important in accounting for the magnitude and volume dependence of the splitting in Fe^{3+} , for example. The second term in (41) is a tensor form involving spin and orbital coordinates and

³³ The compressibility of nickel ferrite is 0.68%/10⁴ kg/cm² [D. F. Gibbons, *J. Appl. Phys.* **28**, 810 (1957)].

³⁴ J. C. Slonczewski, *Suppl. J. Appl. Phys.* **32**, 253S (1961); *J. Phys. Chem. Solids* **18**, 269 (1961).

³⁵ H. A. Bethe and E. E. Salpeter, *Quantum Mechanics of One- and Two-Electron Atoms* (Academic Press, Inc., New York, 1957).

³⁶ R. J. Elliott, *Phys. Rev.* **96**, 266 (1954).

possesses the symmetry of V_{er} . A Hamiltonian of this type has been treated by Sugano and Tanabe.³⁷

Linewidth Mechanism

Considerable insight into the source of thermal relaxation in yttrium iron garnet can be gained from the strain dependence of ferromagnetic resonance. From the pressure dependence of anisotropy, the rate of change of the field for resonance with linear strain induced by hydrostatic stress is

$$|\partial H_{res}/\partial\sigma| \sim 3 \times 10^3 \text{ oe.} \quad (42)$$

A uniaxial stress produces a much larger strain derivative. Geschwind³⁸ finds that the DS_{α}^2 term in the spin Hamiltonian for individual Fe^{3+} ions in yttrium gallium garnet is quite large. This term does not contribute to the anisotropy, however, because of the cubic symmetry of the unit cell. If the unit cell is strained so as to lower the cubic symmetry, these terms can have a profound effect on the anisotropy and field for resonance. A rough measurement by Rowen (unpublished) of the effect of a uniaxial stress gives

$$|\partial H_{res}/\partial\sigma| \sim 4 \times 10^5 \text{ oe,} \quad (43)$$

for the strain derivative.

The distribution of thermal lattice vibrations over

³⁷ S. Sugano and Y. Tanabe, J. Phys. Soc. Japan **13**, 880 (1958).

the sample will give rise to a random spatial fluctuation in the local strain and, hence, the local anisotropy, which in turn will cause a scattering of energy out of the uniform precessional mode. The theory of this source of relaxation would begin with an expansion of the spin Hamiltonian of the system in the phonon and magnon operators. The relaxation could then be discussed in terms of the scattering of $k=0$ magnons by various combinations of magnons and phonons. A detailed theory including this mechanism has been proposed recently by Kasuya and LeCraw.³⁸

Some notion of the size of this interaction may be obtained by considering the x-ray temperature factor data of Geller and Gilleo.³⁹ At room temperature, the root mean square deviation of the separation between O^{2-} and Fe^{3+} is 10% of the average separation. Any calculation, however, must take account of the narrowing effects of the dipole and exchange interactions.

ACKNOWLEDGMENTS

We are indebted to Professor W. Paul for assistance and advice on the high pressure aspects of the experiment and to C. Quadros for growing most of the crystals.

³⁸ T. Kasuya and R. C. LeCraw, Phys. Rev. Letters **6**, 223 (1961).

³⁹ S. Geller and M. A. Gilleo, J. Phys. Chem. Solids **3**, 30 (1957).